Cloud Publications
International Journal of Advanced Packaging Technology
2014, Volume 2, Issue 1, pp. 96-104, Article ID Tech-277
ISSN 2349 – 6665, doi 10.23953/cloud.ijapt.11

Research Article | Open Access

Softwood Pallet Stringer Temperature Estimation

Ali Pourhashemi and Siripong Malasri

Healthcare Packaging Consortium, Christian Brothers University, 650 East Parkway South, Memphis, TN, USA

Correspondence should be addressed to Ali Pourhashemi, apourhas@cbu.edu

Publication Date: 18 June 2014

DOI: https://doi.org/10.23953/cloud.ijapt.11

Abstract Monitoring temperature inside a pallet specimen during a test could be challenging. In this study, two methods were used to estimate temperature in a softwood pallet stringer at the time of testing based on the initial temperature of when it was removed from a temperature chamber and the duration of when it was removed from a chamber until the time it was tested. Five cooling down and three warming up temperature profiles were collected using thermocouples. In the first method, an artificial neural network was developed based on the collected data. In the second method, a mathematical model was suggested based on heat transfer principles. Collected data was used to validate the model. Both methods yield satisfactory results. The heat transfer model allows temperature estimation for specimens with different thickness and species, while the neural network is more precise but limited to the specimen used. Both methods allow other researchers to estimate the temperature without having to collect temperature data.

Keywords *Wooden Pallets; Temperature Estimation; Heat Transfer; Artificial Neural Network*

1. Introduction

In a previous study of the temperature effect on static and impact properties of new softwood pallets [1], static compression tests, drop tests, and incline impact tests were performed at different temperatures ranging from 35 $^\circ F$ to 160 $^\circ F$. Tests could ideally be performed in a temperature-controlled chamber. However, typically these chambers are small. Having large test equipment within a custom-built chamber could be expensive and would risk equipment damages due to extreme temperature. Thus, in this previous study, thermocouples were used to monitor temperatures from the time a specimen was removed from a temperature chamber until it was stabilized at a normal room temperature of 73 ^oF. This stabilizing temperature is considered as the normal test environment by ISTA test protocols, including ISTA Procedure 3A [2]. Equation 1 was developed and used to estimate the temperature inside a specimen at the time of testing:

$$T = \begin{cases} (1.8E-06)t^4 - 0.0006t^3 + 0.0701t^2 - 3.6542t + 160 & \text{for cooling down} \\ (1E-07)t^5 - (3E-05)t^4 + 0.003t^3 - 0.135t^2 + 3.1365t + 32.736 & \text{for warming up} \end{cases} \qquad \text{… Eqn. 1}$$

Where t = time (minutes) and T = temperature (^{o}F). These equations are specific to Yellow Pine stringers, which are widely used in the Southern part of the United States. It was also discussed in the same previous study mentioned above, that the range of temperature in developing a temperature profile has significant effect on a temperature prediction.

This article presents two different methods in estimating temperature based on initial temperature in which a specimen is preconditioned and the time elapsed from the instant it is removed from a temperature chamber to the time of testing. In the first method, an artificial neural network was trained to recognize the temperature data collected from five cooling down and three warming up curves. In the second method, an equation based on heat transfer principles was developed and validated with the collected data.

2. Materials and Methods

2.1. Data Collection

A pallet stringer specimen was placed in a temperature chamber set at different temperatures, i.e., 35 $^{\circ}F$, 45 $^{\circ}F$, 55 $^{\circ}F$, 100 $^{\circ}F$, 120 $^{\circ}F$, 140 $^{\circ}F$, 160 $^{\circ}F$, and 180 $^{\circ}F$ until the temperature at the center of the specimen stabilized. Then it was removed from the chamber and left at room temperature of about 73 $^{\circ}F$. A thermocouple was inserted into the sample. Data was collected at 1-minute intervals through a data acquisition system until it was stabilized at the room temperature. Figure 1 shows the temperature chamber (left) used in the study, a specimen with thermocouples (middle) along with data acquisition system (right). It should be noted that the thermocouple entry points into the specimen were covered with foam (not shown in Figure 1) to avoid heat leakage.

Figure 1: *Data Collection Equipment and Instrumentation [1]*

2.2. Artificial Neural Network

Each cooling down or warming up curve was plotted and fitted with a trend line. The trend line equation was used to generate data for training and validating a neural network. 80% of the generated data was used for training while the remaining 20% was used for validation. A feed-forward, fully-connected back propagation neural network was used with two input cells, sixteen hidden cells, and one output cell, as shown in Figure 2. A bias cell (cell with input of 1) was added to each hidden and output cell. The sigmoid function, $y = \frac{1}{1+e^{-x}}$, was used to generate an output of each hidden and output cell, where x is a weighted sum (sum of the product of a connection weight and the input value going through it) and y is the output of that particular cell.

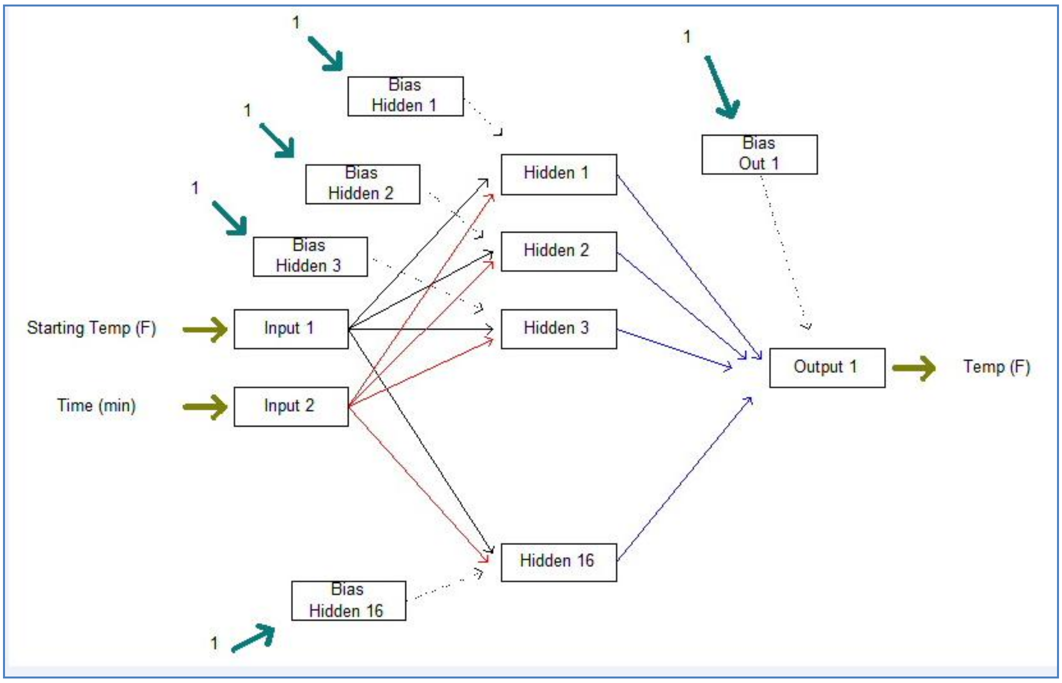

Figure 2: *Neural Network Configuration*

During a training session, errors of predicted values and desired values were minimized through an iterative process of forward and backward passes. Once the errors were at an acceptable level, the network was used to predict the output using only the forward pass for a given set of input figures.

2.3. Heat Transfer Model

Equation 2 is a general heat conduction equation for heat transfer in three dimensions [3].

$$\rho C_p \frac{\partial T}{\partial t} = k\left(\frac{\partial^2 T}{\partial x^2} + \frac{\partial^2 T}{\partial y^2} + \frac{\partial^2 T}{\partial z^2}\right) \qquad \text{… Eqn. 2}$$

Figure 3 shows a sketch of heat conduction in a slab which represents a stringer sample. The specimen thickness (*D*) and depth (*w*) are fixed. The length (*L*) of a specimen of 10 inches was chosen. Since the width is the thinnest part, heat dissipates primarily along this dimension. Thus, this is a one-dimensional flow problem.

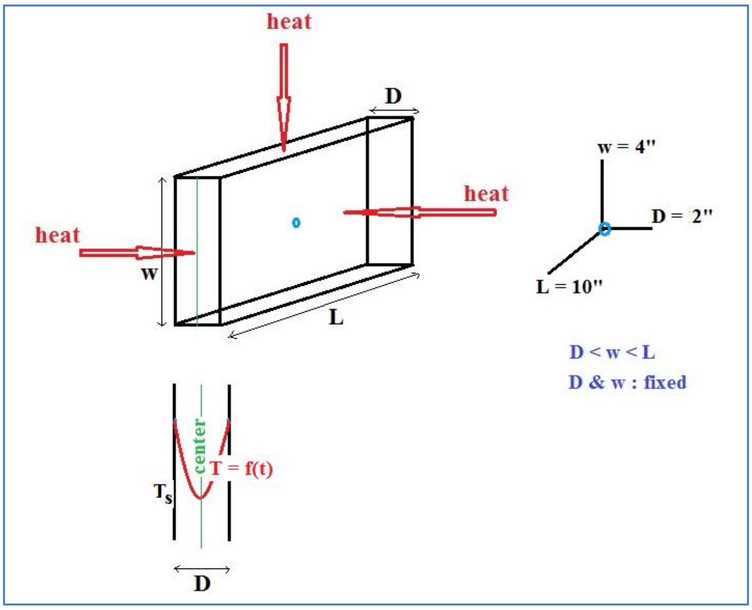

Figure 3: *Heat Conduction in a Slab*

Heat transfer in pallet stringers primarily occurs in one direction, along the thickness which is the thinnest part. Thus, Equation 2 can be reduced to:

$$\rho C_p \frac{\partial T}{\partial t} = k\left(\frac{\partial^2 T}{\partial x^2}\right) \qquad \text{… Eqn. 3}$$

Where ρ = density (kg/m^3), C_p = heat capacity (J/kg·K), k = thermal conductivity (W/m·K), T = temperature ($^\circ F$), and t = time (minutes).

Density (ρ), heat capacity (C_p), and thermal conductivity (k) were assumed to be constant during the heat transfer process due to a small temperature range. The surface temperature (T_s), which is the room temperature during the warming up or cooling down was also constant, while at the center of the specimen ($x = 0$) the heat transfer rate, $\frac{dT}{dx}$ was zero. The final one-dimensional, unsteady-state heat conduction model was suggested according to [3]:

$$T(x,t) := T_s + \frac{2(T_0 - T_s)}{\pi}\sum_{n=1}^{200}\left[\left(\sin(x\cdot\beta(n))\right)\cdot e^{-\left[\alpha t(\beta(n))^2\right]}\left[\frac{1-(-1)^n}{n}\right]\right] \qquad \text{... Eqn. 4}$$

Where L = thickness of the specimen (inches), x = local distance from the center (inches), T = transient temperature ($^\circ F$), T_0 = initial temperature ($^\circ F$), T_s = final room or the surface temperature ($^\circ F$), t = time (minutes), α = thermal diffusivity (m/s^2) = $\frac{k}{\rho}C_p$, β(n) = Eigen value (m^{-1}) = $n\frac{\pi}{L}$ and n =1, 2, 3…..

3. Results and Discussion

3.1. TempNet: A Neural Network for Temperature Estimation

Trend line equations, shown in Table 1, were generated from the collected data. It should be noted that these trend lines change the starting temperature somewhat, such as 56 $^\circ F$ instead of 55 $^\circ F$ and 165 $^\circ F$ instead of 160 $^\circ F$. In these equations, x is time (minutes) and y is temperature ($^\circ F$).

Table 1: *Trend Line Equations*

Trend Line Equations	R^2
$y_{188} = -0.0002x^3+0.0507x^2-3.892x+187.75$	0.9983
$y_{165} = -0.0002x^3+0.046x^2-3.3304x+165.18$	0.9979
$y_{142}= -0.0001x^3+0.0282x^2-2.3376x+142.41$	0.9977
$y_{123} = -9E-05x^3+0.0214x^2-1.6869x+123.34$	0.9965
$y_{103} = -5E-05x^3+0.0116x^2-0.9459x+102.9$	0.9922
$y_{56} = 4E-05x^3-0.0086x^2+0.6485x+55.627$	0.9837
$y_{45} = 5E-05x^3-0.0114x^2+0.9178x+45.417$	0.9916
$y_{35} = 7E-05x^3-0.0157x^2+1.1888x+35.128$	0.9935

A total of 248 examples generated from these trend lines (shown in Figure 4 and Table 2) are used in the neural network development. Out of the 248 examples, 199 were used in training the network (seen data) and 49 were used in validating the network (unseen data).

NeuroShell 2 [4] was used to train the neural network using training parameters shown in Figure 5. The performance of the network in terms of error percentage of the desired output is summarized in Table 3. The software also generated a generic source code as shown in Appendix A. A spreadsheet, TempNet [5], was then developed following the logic given in this generic source code as shown in Figure 6. In addition, two starting temperatures not part of the collected data, represented by the two solid-line graphs in Figure 7, were used to test the network ability to generalize, i.e., interpolation between graphs from collected data. It is clear that the network has ability to recognize the patterns of how temperature changes with time.

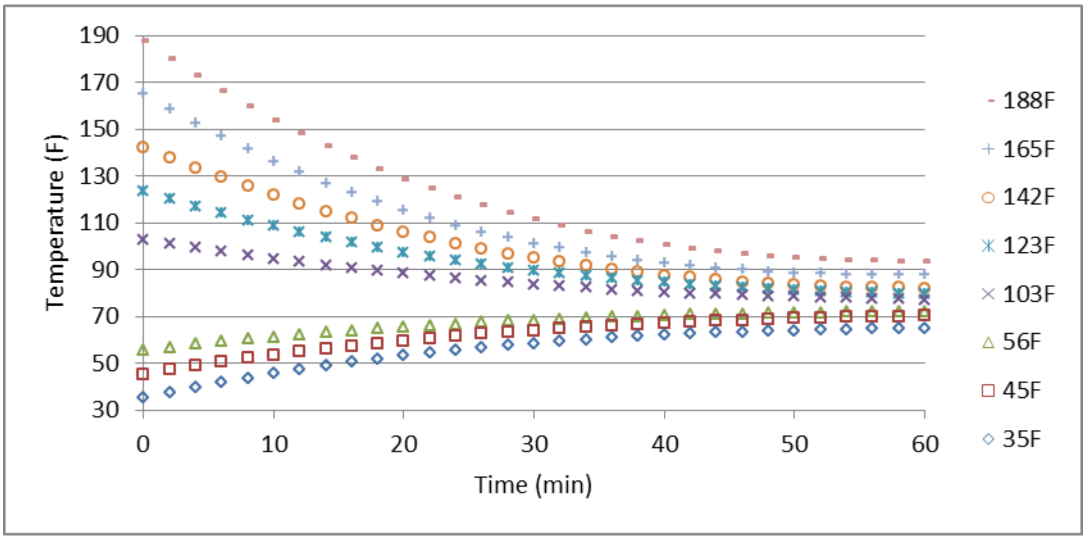

Figure 4: *Data for Network Development*

Table 2: *Training Data (T) and Validation Data (V)*

START	TIME	TEMP	MARK	NOTES
35	0	35	T	T = Training (Seen Data)
35	2	37	T	
35	4	40	T	
35	6	42	T	
35	8	44	V	V = Validation (Unseen Data)
35	10	46	T	
35	12	47	T	
35	14	49	T	
188	50	95	T	
188	52	94	T	
188	54	94	V	
188	56	94	T	
188	58	94	T	
188	60	94	T	

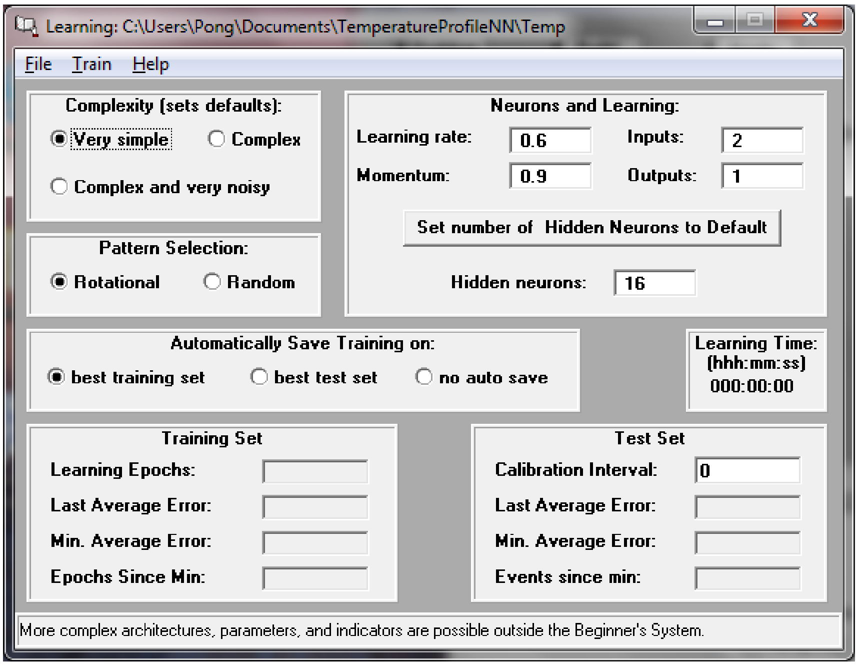

Figure 5: *Network Training Parameters*

Table 3: *Network Performance*

Group	Seen Data (T)	Unseen Data (V)	All Data (T + V)
Number of Examples	199	49	248
Minimum Error (%)	0.01	0.04	0.01
Maximum Error (%)	5.76	3.89	5.76
Average Error (%)	1.23	1.15	1.21

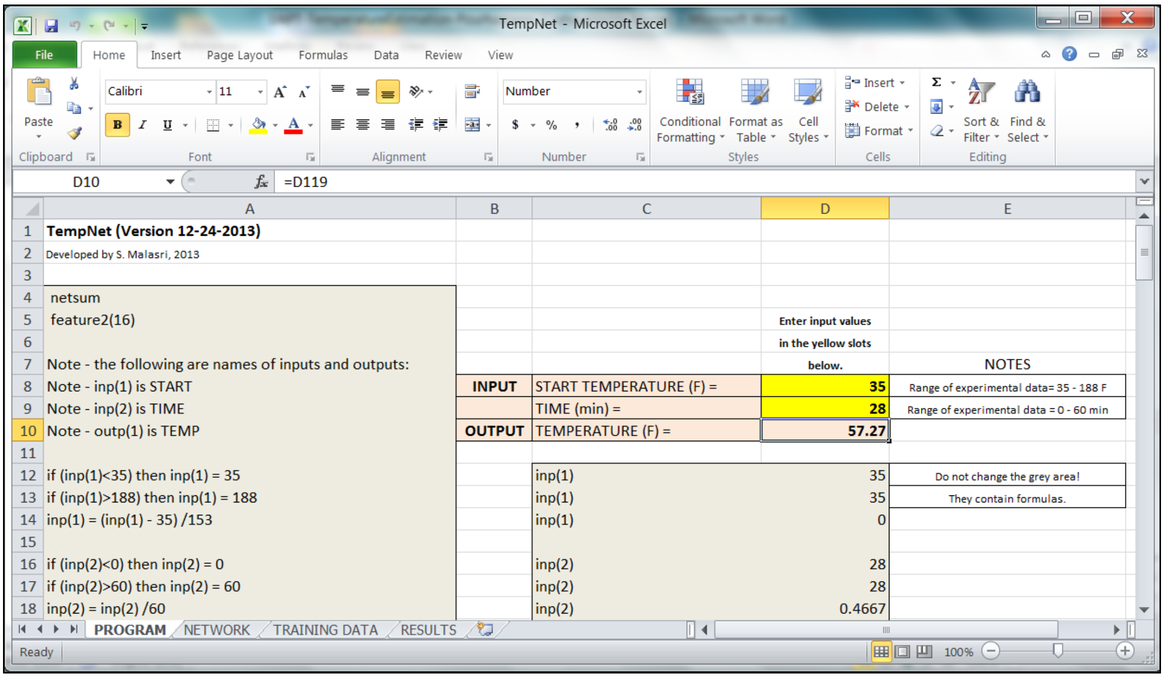

Figure 6: *TempNet Spreadsheet [5]*

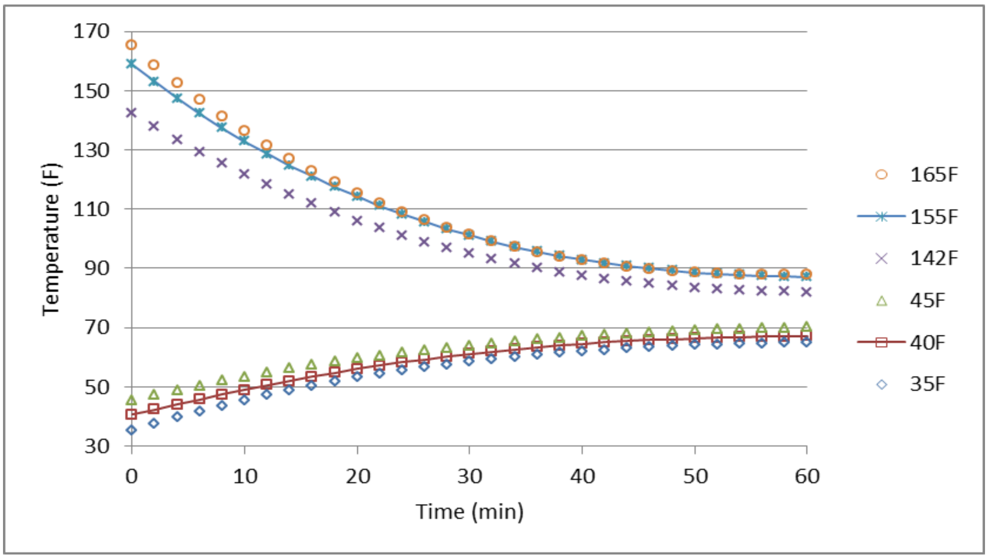

Figure 7: *Network Ability to Interpolate Between Know Values*

3.2. Heat Transfer Model

The heat transfer model presented earlier was used to estimate temperature. Comparison was made with actual collected data in Figure 8. Using the physical properties [6], the model-predicted temperature profiles were compared with the experimental data for various temperature settings. The equation was verified for various initial temperature settings and only one setting (T_o= 180 °F) is presented in this paper. Overall, the model-predicated temperatures have shown a close agreement with the experimental data for all surface temperature settings (T_s = room temperature) and depths. The over prediction of temperature in the early transient period was due to assumption of a high constant surface temperature in the equation. For example, Figure 9 compares the theoretical T_s with the experimental data as it reaches steady state. The experimental T_s is not constant during the transient period, but it recovers gradually and it reaches to about 70% of the final temperature within 15 minutes. Although the difference between the experimental and the theoretical T_s seems noticeable in Figure 9, the predicted temperatures of inner layers are within acceptable range as shown by a 10% error bar in Figure 8. One may also argue that assumption of a natural convective boundary condition rather than constant T_s at the surface may improve the accuracy of the temperature prediction of the inner layers, but this requires detailed calculation of the heat transfer coefficient (i.e., f (Gr no. and Pr. no)) at various surrounding conditions which is not required for this work and its practical application. Therefore, assumption of a constant surface temperature provides sufficient ability to predict the temperature data with about 90% accuracy in most cases. (Legends: Gr no: Grashof number, Pr no: Prandtl number)

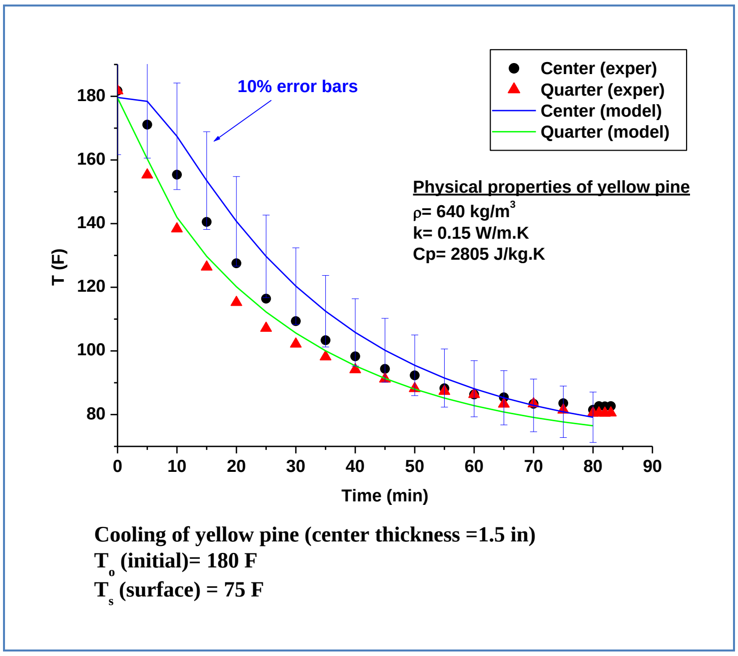

Figure 8: *Comparison of Temperature Profiles (Experimental vs. Model)*

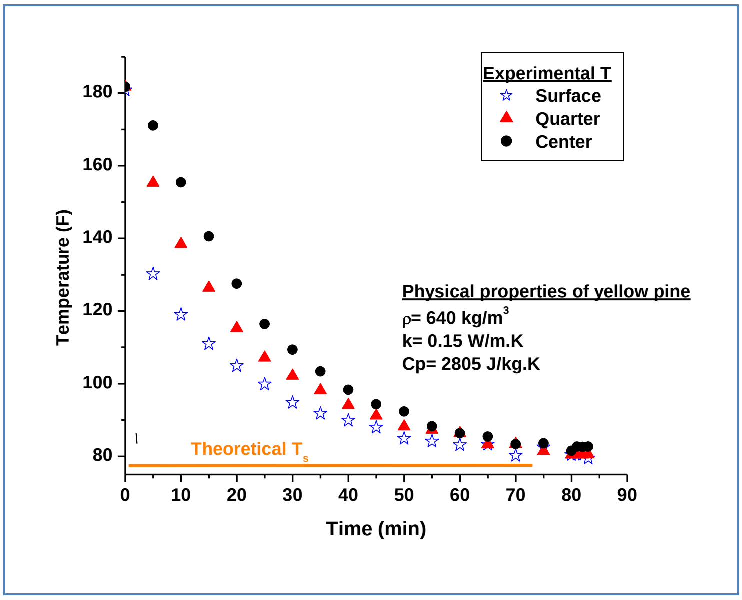

Figure 9: *Comparison of Experimental and Theoretical Surface Temperatures*

4. Conclusion

Both methods give effective predictions of the temperature inside the specimen. The neural network model is quite accurate since it was developed based on the collected data. However, it is limited to the Yellow Pine pallet stringers with a 2-inch thickness. The heat transfer model is less accurate but can be applied to different species of wood and thickness. The two models presented will eliminate the time-consuming data collections and manipulation for determination of pallet temperature.

References

[1] Malasri, S., Pourhashemi, A., Brown, R.W., Harvey, M., Moats, R., Godwin, K., Aung, P., and Laney, J. *Effect of Temperature on Static and Impact Properties of New Softwood Pallets*, International Journal of Advanced Packaging Technology. 2013. 1 (1) 30-39.

[2] ISTA Procedure 3A, 2008: *Packaged-Products for Parcel Delivery System Shipment 70 kg (150 lb) or Less*. International Safe Transit Association, East Lansing, MI.

[3] Hohn, D.W., Ȍzisik, M.N., 2012: Heat Conduction. John Wiley & Sons Inc.

[4] Ward Systems Group, Inc. *NeuroShell 2*. http://www.wardsystems.com/neuroshell2.asp (As of December 31, 2013)

[5] Malasri, S. *Packaging e-materials*. http://facstaff.cbu.edu/pong/e-Materials.html (As of May 4, 2014)

[6] Incropera, F.P., and DeWitt, D.P., 2002: *Heat and Mass Transfer*. 5th Ed. John Wiley & Sons.